

# Connecting the Convective Mach Number to Full-scale Supersonic Jet Noise Directivity

Matthew A. Christian<sup>1</sup>, Kent L. Gee<sup>2</sup>  
*Brigham Young University, Provo, Utah, 84602*

This paper describes investigations into convective Mach number and its relationship to maximum radiation angle for an installed afterburner-capable military jet engine. The convective Mach number describes the velocity of coherent structures in the turbulent mixing layer of a jet. For supersonic jets, this parameter should be useful in predicting the maximum noise radiation angle. However, of the several definitions of the convective Mach number, none have been successful in predicting the peak radiation angle of all jets. In this paper, physics-based and empirically derived convective Mach numbers are calculated from data collected from a T-7A-installed GE F404 engine and are compared against measured maximum noise directivity angles. Of the physics-based definitions, the T-7A data show the convective Mach number associated with Oertel’s first family of instability waves predicts the maximum radiation angle within 6° over a range of engine conditions. Additionally, the so-called “Oertel convective Mach number,” which has successfully predicted peak directivity angles in rocket noise studies, is a relatively poor predictor of the T-7A maximum directivity angle. An empirical formulation of the convective Mach number suggests that, for the T-7A, the “convective velocity” of coherent structures in the shear layer is about 60% of the fully-expanded centerline velocity for supersonic engine conditions. Evaluating this empirical definition of the convective Mach number using data from other jet noise studies shows that the acoustic Mach number appears to be the best predictor of the convective velocity. Finally, a frequency-dependent study of the convective Mach number at afterburner shows the peak directivity angle is roughly constant at low and high frequencies, while the frequencies associated with the transition from the potential core to the supersonic core show the greatest change in directivity.

## I. Nomenclature

AB	=	Afterburner
$c_a$	=	Ambient sound speed
$c_j$	=	Fully-expanded sound speed
$D_j$	=	Fully-expanded jet diameter
$\kappa$	=	Empirically derived coefficient
MARP	=	Microphone array reference point
$M$	=	Mach number
$M_{ac}$	=	Acoustic Mach number
$M'_c$	=	Convective Mach number for the first family of instability waves
$M_c$	=	Convective Mach number for the second family of instability waves
$M''_c$	=	Convective Mach number for the third family of instability waves
$M_j$	=	Fully-expanded Mach number
MWR	=	Mach wave radiation
OASPL	=	Overall sound pressure level
$\theta_{Max}$	=	Maximum noise directivity angle
SPL	=	Sound pressure level

<sup>1</sup> Graduate Student, Department of Mechanical Engineering, AIAA student member

<sup>2</sup> Professor of Physics, Department of Physics and Astronomy, AIAA Associate Fellow

$Sr$	=	Strouhal number
$U_c$	=	Convective velocity
$U_j$	=	Fully-expanded jet velocity
$w'$	=	Velocity of the first family of instability waves
$w$	=	Velocity of the second family of instability waves
$w''$	=	Velocity of the third family of instability waves

## II. Introduction

Early characterizations of turbulent mixing layers showed that large coherent structures form within the mixing layer [1–4]. These structures travel downstream at some convective velocity ( $U_c$ ). Bogdanoff [5] developed a Mach number to describe the velocity of these structures, later referred to as the convective Mach number by Papamoschou and Roshko [6]. The convective Mach number has been of particular interest in the field of jet acoustics for predicting the directivity of supersonic jet noise, where Mach wave radiation (MWR) is the dominant noise source [7–9]. The presumed link between the convective Mach number and the maximum radiation directivity angle ( $\theta_{Max}$ ) can be found using the familiar Mach angle relation:

$$\theta_{Max} = 180^\circ - \cos^{-1}\left(\frac{1}{M}\right), \quad (1)$$

where  $M$  represents a generic Mach number and  $\theta_{Max}$  is measured with respect to the jet inlet axis. How the convective Mach number is calculated, however, has varied between researchers, with no one definition seeming to accurately predict the peak radiation angle of all supersonic jet sources.

Definitions of the convective Mach number have typically been either physics-based or empirically derived. The physics-based definitions of the convective Mach number explored here are based on the important findings of Oertel [10], who experimentally found that Mach waves from a supersonic jet favor three distinct velocities,  $w' > w > w''$ . These velocities are each associated with a distinct family of instability waves. The first family,  $w'$ , are the familiar Kelvin-Helmholtz instability waves and have been associated with a strong acoustic field [11]. The second family of instability waves,  $w$ , are referred to as “supersonic instability waves.” These waves produce noise whenever the jet velocity is greater than the sum of the jet and ambient sound speeds [12]. The third family,  $w''$ , are referred to as subsonic instability waves and are contained within the jet [11]. Organizing these three families of Mach wave velocities into unique convective Mach numbers gives [12]:

$$M'_c = \frac{U_j + c_j}{c_j + c_a}, \quad (2)$$

$$M_c = \frac{U_j}{c_j + c_a}, \quad (3)$$

$$M''_c = \frac{U_j - c_j}{c_j + c_a}. \quad (4)$$

In these equations,  $U_j$  is the fully-expanded jet velocity, and  $c_j$  and  $c_a$  are the fully-expanded and ambient sound speeds, respectively.

Because  $w''$  has been shown to have little effect on the acoustic field for jets with fully-expanded Mach numbers below 2, Greska [13] opted to link the overall noise radiation to the first two families of waves, Eq. (2) and Eq. (3), by taking their arithmetic mean. This new parameter was dubbed the Oertel convective Mach number, honoring the work done by Oertel. The resulting relation is given as:

$$M_{c,O} = \frac{U_j + \frac{1}{2}c_j}{c_j + c_a}. \quad (5)$$

The Oertel convective Mach number has recently been used to predict maximum directivity angles from rocket static firing and launch measurements. James et al. [14], Hart et al. [15], and Bassett et al. [16] each showed that the Oertel convective Mach number predicted the peak directivity angle of different rockets within just a couple of degrees.

Stepping aside from the theoretical models used to predict convective velocities, many jet aeroacoustics studies have used an empirical definition for the convective Mach number ( $M_{c,\kappa}$ ), defined here as,

$$M_{c,\kappa} = \kappa \frac{U_j}{c_a}. \quad (6)$$

Using Eq. (1), the measured  $\theta_{Max}$  is used to calculate an appropriate  $\kappa$ . Conceptually,  $\kappa$  can be described as the ratio of  $U_c$  to  $U_j$ . Values for  $\kappa$  vary based on the application. For laboratory-scale supersonic jets, researchers have suggested  $\kappa$  values between 0.6 and 0.8 for various jet parameters [12,18–20], while rocket noise research has shown values closer to 0.3 are more appropriate [15–17].

Using acoustic data and jet parameters from a T-7A-installed GE F404 engine, this paper compares physics-based and empirical definitions of the convective Mach number against measured maximum directivity angles. To better understand the variability of  $\kappa$  values between jets at different operating conditions,  $\kappa$  is calculated for the T-7A at four engine conditions. These values are compared against a database of jet parameters compiled from several published supersonic jet noise studies, ranging from laboratory-scale jet noise measurements to measurements of rocket launches. Values for  $\kappa$  calculated from these data, along with the T-7A  $\kappa$  values, are shown as a function of their temperature ratio, fully-expanded Mach number, and the acoustic Mach number. Finally, frequency-dependent convective Mach numbers are explored and connected with jet source phenomena.

### III. Data Collection

The Boeing/Saab T-7A “Red Hawk” is a supersonic trainer aircraft developed for the United States Air Force, equipped with a single F404-GE-103 jet engine. Acoustic measurements were made of a T-7A-installed F404 engine at Holloman Air Force Base, New Mexico on August 18<sup>th</sup>, 2019. During the measurement, the aircraft was tied down on a run-up pad with the front of the aircraft facing the jet blast deflector. This unique orientation was implemented to preserve the jet as far downstream as possible. The aircraft was then run at idle, 75% N2, 82% N2, 88% N2, military power (MIL), and afterburner (AB) engine conditions for 30 seconds each. This paper will only include analyses of the four highest engine powers. The run-up cycle was completed six times throughout the measurement. Significant differences were observed in spectral nulls of the first two runs compared to the last four, a phenomenon currently attributed to a changing temperature gradient that occurred around sunrise. Rather than trying to account for this discrepancy, only the data collected during the last four runs will be used in this paper.

The measurement consisted of over 200 microphones arranged in both the acoustic near and far fields. This paper focuses on just two of the far-field arcs, one at 38 m (125 ft) and the other at 76 m (250 ft). The 38 m arc was made up of 14 1/4" GRAS 40BD microphones, while the 76 m arc had 22 1/4" GRAS 46BD microphones. All microphones were arranged relative to the microphone array reference point (MARP), located 4 m (13 ft) downstream of the nozzle. Angles are oriented such that 0° is in front of the aircraft, and 180° is directly behind the aircraft. As seen in Fig. 1, the microphones in the 38 and 76 m arc were arranged at inlet angles from 30° to 160° in 10° increments, with additional microphones in 5° increments between 30° and 60° and again between 110° and 160° in the 76 m arc. Due to a loose connection, data from the 130° microphone in the 76 m arc were corrupted and will not be included in any analysis.

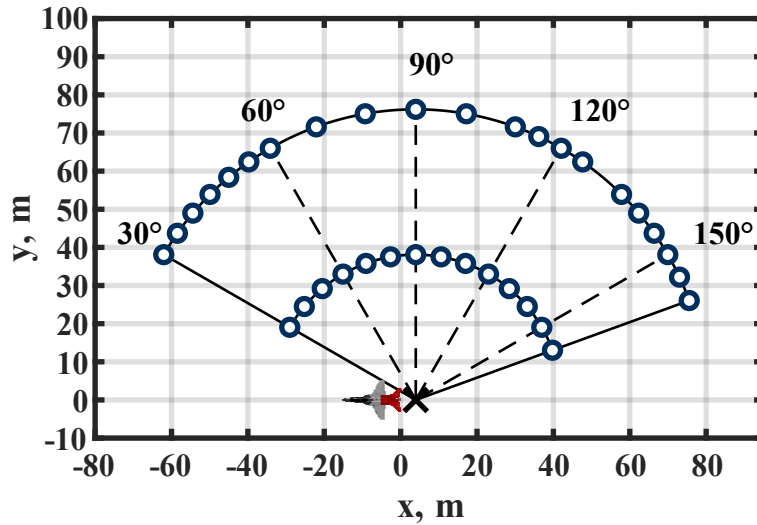


Fig. 1: Schematic of 38 m and 76 m far-field microphone arrays.

Microphones were connected via InfiniBand and BNC cables to a National Instruments PXIe-1062 chassis with 4496 cards as well as an NI 8840 Quad-Core Controller. For the four runups described here, the data were synchronously sampled at 96 kHz. Further information regarding the data acquisition process is found in Leete et al. [21]. Of the considered engine powers, the fully expanded jet velocity was found to be subsonic at 82% N<sub>2</sub>, slightly supersonic at 88% N<sub>2</sub>, and well within the supersonic regime at MIL and AB.

Because this measurement took place outdoors, multi-path interference from ground reflections significantly affects the measured acoustic data. To account for this, the model described by Gee et al. [22] is implemented for all presented T-7A data. This model attempts to remove the effects of ground reflections on measured spectra by accounting for source and receiver geometry, a finite impedance ground, and a turbulent atmosphere. Information regarding the implementation of this model for the T-7A data is not described here for the sake of brevity but can be found in Christian et al. [23].

## IV. Analysis

### A. Convective Mach Number Calculations from T-7A Measurement

Figure 2 shows the overall sound pressure level (OASPL) directivity curves generated from the T-7A data at four different engine conditions. The markers represent the levels measured by the mics, while the lines connecting them represent the levels interpolated using MATLAB's *pchip* function, a shape-preserving piecewise cubic interpolation method. Note the maximum radiation inlet angle decreases as the engine power increases.

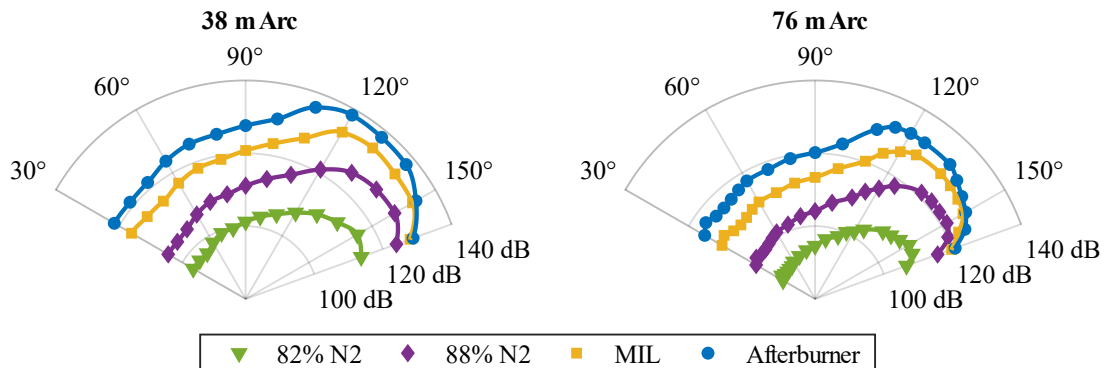


Fig. 2: OASPL directivity curves at the four highest engine conditions measured at both far-field arcs.

Table 1 provides values obtained for different definitions of the convective Mach number using the T-7A data. These convective Mach numbers are then used to predict a peak radiation angle using Eq. (1). These predicted angles, given in parentheses next to their accompanying convective Mach number, are compared against the measured  $\theta_{Max}$ . Note that for subsonic convective Mach numbers there is no peak radiation angle. Table 1 also shows the values for  $\kappa$  calculated from the measured  $\theta_{Max}$  using the relation,

$$\kappa = \frac{-c_a}{U_j \cos(\theta_{Max})}. \quad (7)$$

**Table 1: Calculated convective Mach number values and their predicted angles from T-7A data compared against the measured peak radiation angle.**

Engine Power	$M_j$	$M'_c$	$M_c$	$M''_c$	$M_{c,O}$	$\kappa$	$\theta_{Max}$
<b>AB</b>	1.46	1.70 (126°)	1.01 (171°)	0.32 (N/A)	1.36 (137°)	0.60	120°
<b>MIL</b>	1.43	1.48 (132°)	0.87 (N/A)	0.26 (N/A)	1.18 (148°)	0.62	135°
<b>88% N2</b>	1.10	1.23 (144°)	0.64 (N/A)	0.04 (N/A)	0.93 (N/A)	0.81	140°
<b>82% N2</b>	0.94	1.15 (150°)	0.56 (N/A)	-0.02 (N/A)	0.86 (N/A)	0.86	150°

$M'_c$  (see Eq. (2)) is shown to be supersonic at each of the four engine conditions, including at 82% N2 where the fully-expanded Mach ( $M_j = U_j/c_j$ ) number is subsonic.  $M'_c$  accurately predicts  $\theta_{Max}$  at 82% N2 within a fraction of a degree. The presence of MWR at subsonic fully-expanded conditions was also observed and discussed by Greska [13], who showed such a condition was possible for a sufficiently heated jet. This accuracy drops with increasing engine power, with a difference of 4° at 88% N2, 3° at MIL, and 6° at AB. Because  $M_c$  and  $M''_c$  are subsonic, even at AB conditions, the jet velocity is not large enough for  $M_c$  or  $M''_c$  to have an impact on the sound field. These results indicate that the only family of instability waves that significantly contribute to the acoustic field are the Kelvin-Helmholtz instability waves. This agrees with Greska [13] who explained that  $w''$  only occurs at the most supersonic jet velocities, and Seiner et al. [12] who observed that  $w$  is only present at sufficiently high jet Mach numbers and plume temperatures.

This could explain why the Oertel convective Mach number,  $M_{c,O}$ , would be more useful in rocket noise studies where the jet velocity is much greater.  $M_{c,O}$  at both AB and MIL predicts angles much greater than what was measured and is subsonic for the other two engine conditions, suggesting that this definition is not useful for predicting the peak radiation angle of afterburning jet engines. This conclusion is contrasted with the results of Hart et al. [15] and Bassett et al. [16] who both used  $M_{c,O}$  to predict maximum directivity angles for the Delta IV Heavy vehicle and the GEM-63 booster that were within 1° of their measured  $\theta_{Max}$ .

## B. Connecting $\kappa$ to Jet Parameters

One drawback of the empirical definition  $M_{c,\kappa}$ , given in Eq. 6, is the varied values of  $\kappa$  given by different authors. For laboratory-scale jets, values between 0.6 and 0.8 have been reported [12,18,19,24,25], while values given in rocket noise literature have been closer to 0.3 [15,17]. The velocities and temperatures from rockets are significantly greater than those seen in laboratory-scale or even full-scale jets, but whether the variability in  $\kappa$  is due to the increase in velocity or temperature is not well understood. To investigate this, the reported jet and acoustic parameters from eight papers [12–15,17,20,26,27] were collected into a single database. From these values, a  $\kappa$  value was calculated using Eq. 7.

In Figs. 3-5, data from laboratory-scale jets are represented as circles, rocket data are given as squares, and the T-7A data are given as red triangles. From these combined data, a simple logarithmic curve fit is employed,

$$\kappa = A + B \log_{10} \beta, \quad (8)$$

where  $\beta$  is some independent variable and  $A$  and  $B$  are the coefficients calculated using MATLAB's "fit" function. The independent variables evaluated here are  $M_j$ , TTR, and the acoustic Mach number,  $M_{ac}$ , defined as,

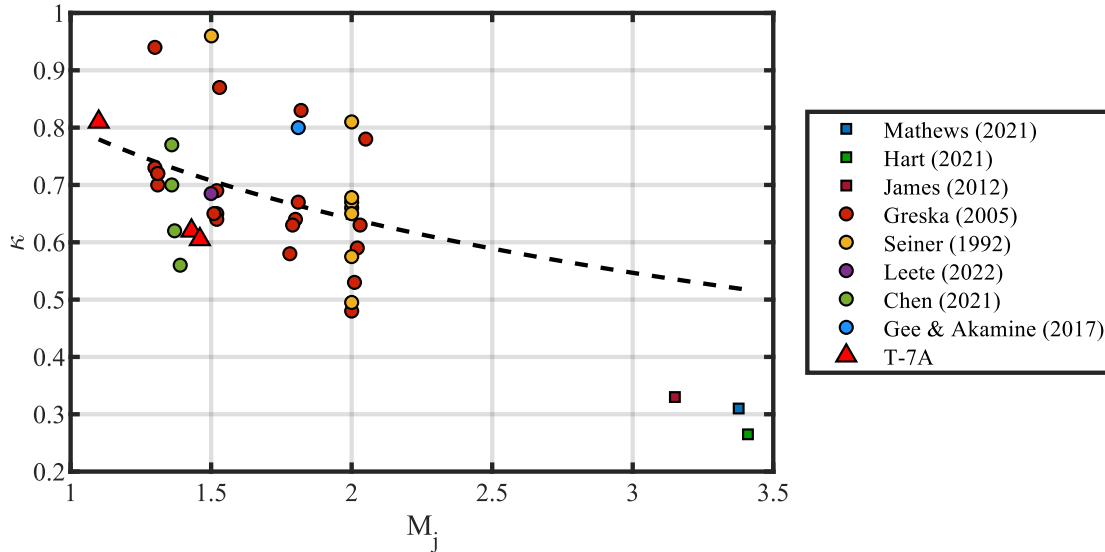
$$M_{ac} = \frac{U_j}{c_a}. \quad (9)$$

In all cases,  $c_a$  is assumed to be constant at room temperature. The resulting regression curves are represented in Figs. 3-5 as a dashed line. The calculated coefficients for each of the independent variables along with each curve's  $R^2$  value is given in Table 2.

**Table 2: Logarithmic curve fitting coefficients and  $R^2$  values.**

Independent Variable	$A$	$B$	$R^2$
$M_j$	0.80	-0.23	0.20
TTR	0.83	-0.15	0.67
$M_{ac}$	0.91	-0.29	0.87

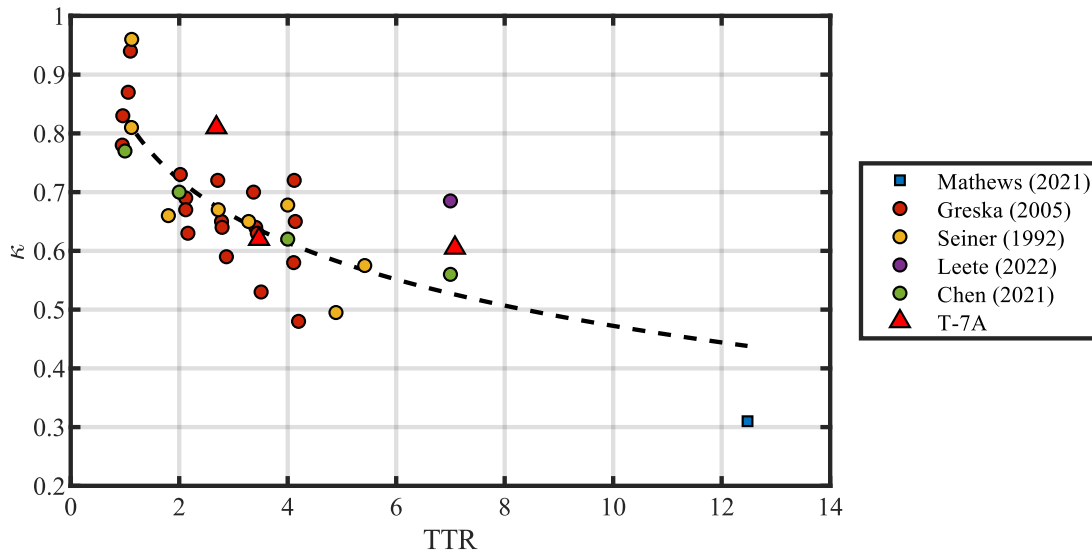
Starting with the parameter with the smallest  $R^2$  value, Fig. 3 shows  $\kappa$  as a function of the fully expanded Mach number ( $M_j$ ).



**Fig. 3:  $\kappa$  given as a function of  $M_j$  with logarithmic regression curve given as dashed line ( $R^2 = 0.20$ ).**

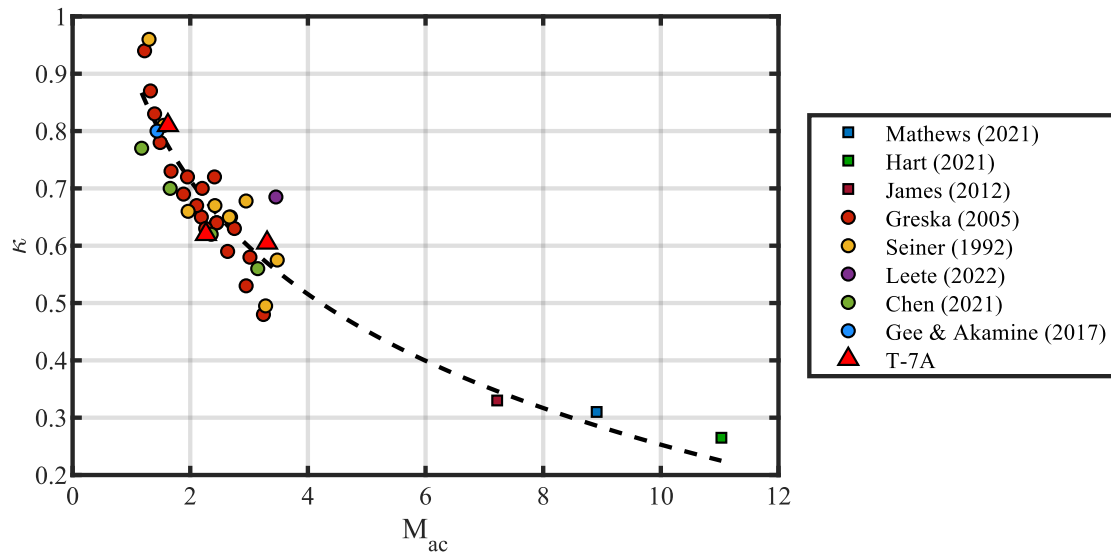
From the compiled dataset, Greska [13], Seiner et al. [12], and Chen et al. [20] each measured jets with the same  $M_j$ , but with varying temperature ratios. In Fig. 3, these measurements show varied  $\kappa$  values at the same or similar  $M_j$ , which would indicate a weak, if any, dependence of  $\kappa$  on  $M_j$ .

Figure 4 shows  $\kappa$  as function of the total temperature ratio (TTR, defined as the ratio of the stagnation temperature to the ambient temperature). Table 2 shows  $R^2 = 0.67$  for the curve in Fig. 4. While this could mean a stronger dependence of  $\kappa$  on TTR relative to  $M_j$ , values from Greska [13] show large changes in  $\kappa$  with relatively small changes in TTR. This indicates that, while  $\kappa$  may have some dependence on TTR, there are other factors in play.



**Fig. 4:  $\kappa$  given as a function of TTR with logarithmic regression curve given as dashed line ( $R^2 = 0.67$ ).**

Figure 5 shows  $\kappa$  as a function of  $M_{ac}$ . This shows the best collapse of data of all the considered variables. An  $R^2$  value of 0.87 suggests a much greater dependence on  $M_{ac}$  as opposed to TTR or  $M_j$ . The database used here is limited but provides a starting point for further study on the effects of jet parameters on convective velocity. Additional research is needed to better analyze the effects of jet parameters on radiation directivity. Assuming the trend shown here continues, it would be expected that  $M_{ac}$  would be the best indicator of the peak radiation angle, with the jet temperature ratio having a relatively smaller impact on the peak angle.



**Fig. 5:  $\kappa$  given as a function of  $M_{ac}$  with logarithmic regression curve given as dashed line ( $R^2 = 0.87$ ).**

### C. Frequency-dependent Effects

To examine the frequency-dependent relationship between directivity and the convective Mach number,  $\kappa$  values can be calculated from one-third octave band frequency-dependent directivity curves. Figure 6 shows  $\kappa$  values calculated using peak radiation angles from one-third octave band frequency directivity curves at AB. For scaling purposes, the x-axis in Fig. 6 is given as a Strouhal number (Sr), defined here as,

$$\text{Sr} = \frac{fD_j}{U_j}, \quad (10)$$

where  $D_j$  is the fully-expanded diameter and  $f$  is frequency.

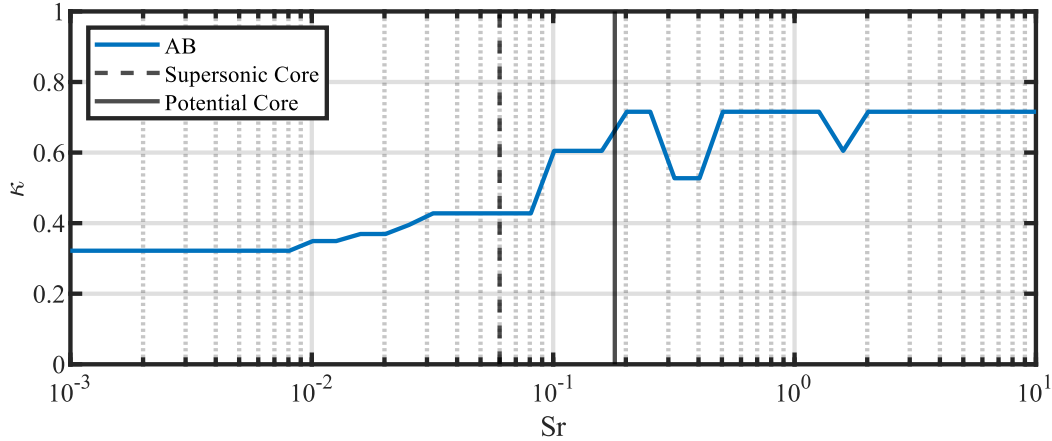


**Fig. 6:  $\kappa$  values calculated from frequency-dependent peak directivity angles at AB.**

There appear to be three distinct regions where  $\kappa$  is either relatively constant or growing. Moving from low to high Sr, the first region is contained between Sr values of  $10^{-3}$  and  $2 \cdot 10^{-2}$ , where  $\kappa$  is constant at  $\sim 0.32$ . The second region is where  $\kappa$  increases from 0.32 to 0.7 between  $2 \cdot 10^{-2}$  and  $2 \cdot 10^{-1}$ . The final region is for  $\text{Sr} > 2 \cdot 10^{-1}$ , and, while there are some dips,  $\kappa$  is roughly constant at  $\sim 0.7$ .

This change in  $\kappa$  with Sr indicates a change in directivity at different frequencies. This phenomenon can be clearly seen in the near-field acoustical holography-based field reconstructions done by Mathews et al. [28] from the same T-7A measurement. Their apparent source spatio-spectral reconstructions at the nozzle lip line at AB show that most high Sr noise is generated closer to the nozzle exit, with lower Sr noise being generated further downstream. Superimposing the calculated potential and supersonic core lengths on their spatio-spectral reconstruction showed the peak Sr to be  $\sim 0.18$  at the potential core length and  $\sim 0.06$  at the supersonic core length. These Sr values are represented in Fig. 6 as vertical lines, solid for the potential core length and dashed for the supersonic length, and they roughly bound the region in the spectrum where  $\kappa$  sees the most growth. Connecting this spectrum with the physical jet, the third region appears to be related to the supersonic region of the jet, upstream of the potential core tip, where the peak directivity angle is constant and pointed more to the sideline. The first region would then correspond to the subsonic region downstream of the supersonic core length, where the peak directivity is again roughly constant, but more downstream.

## V. Conclusion

The convective Mach number is a parameter that can be useful in predicting the peak noise radiation angle of a supersonic jet. This paper compares definitions of the convective Mach number against measured peak directivity angles from a T-7A-installed GE F404 engine. These observations were connected back to the three families of instability waves found by Oertel, and it appears that only Kelvin-Helmholtz instability waves affect the peak radiation angle of the T-7A. The Oertel convective Mach number, which has been useful in predicting peak radiation angles of rockets, was shown to consistently over-predict the peak radiation angle of the T-7A.

The empirically derived parameter  $\kappa$ , which is the ratio of  $U_c$  to  $U_j$ , was calculated to be  $\sim 0.6$  at supersonic engine conditions. Values for  $\kappa$  were calculated from jet parameters and peak noise radiation angles reported in eight different studies of rocket and laboratory-scale jet noise. Comparing these calculated  $\kappa$  values against various jet parameters, it was found that  $M_{ac}$  was the strongest predictor of the  $\kappa$  value. The spectral analysis in this paper shows that  $\kappa$  generally increases with the Strouhal number. Finally,  $\kappa$  values were calculated from frequency-dependent directivity curves.

The resulting  $\kappa$  spectrum showed that, at AB, the peak directivity angle was roughly constant at low and high Sr numbers. Additionally, the peak Sr values at the potential and supersonic core lengths roughly bound the region where the  $\kappa$  values change most rapidly.

## References

- [1] Crow, S. C., and Champagne, F. H. "Orderly Structure in Jet Turbulence." *J. Fluid Mech.*, Vol. 48, No. 3, 1971, pp. 547–591.
- [2] Brown, G. L., and Roshko, A. "On Density Effects and Large Structure in Turbulent Mixing Layers." *J. Fluid Mech.*, Vol. 64, No. 4, 1974, pp. 775–816.
- [3] Winant, C. D., and Browand, F. K. "Vortex Pairing: The Mechanism of Turbulent Mixing-Layer Growth at Moderate Reynolds Number." *J. Fluid Mech.*, Vol. 63, No. 2, 1974, pp. 237–255.
- [4] Hussain, A. K. M. F. "Coherent Structures and Turbulence." *J. Fluid Mech.*, Vol. 173, 1986, pp. 303–356.
- [5] Bogdanoff, D. W. "Compressibility Effects in Turbulent Shear Layers." *AIAA J.*, Vol. 21, No. 6, 1983, pp. 926–927.
- [6] Papamoschou, D., and Roshko, A. "The Compressible Turbulent Shear Layer: An Experimental Study." *J. Fluid Mech.*, Vol. 197, 1988, pp. 453–477.
- [7] Liu, J., Corrigan, A., Kailasanath, K., and Taylor, B. "Impact of the Specific Heat Ratio on the Noise Generation in a High-Temperature Supersonic Jet." *AIAA Paper 2016-2125*, 2016.
- [8] Vaughn, A. B., Gee, K. L., Swift, S. H., Leete, K. M., Wall, A. T., Downing, J. M., and James, M. M. "Source Localization of Crackle-Related Events in Military Aircraft Jet Noise." *AIAA J.*, Vol. 59, No. 6, 2021, pp. 2251–2261.
- [9] Leete, K. M., Wall, A. T., Gee, K. L., Neilsen, T. B., James, M. M., and Downing, J. M. "Acoustical Holography-Based Analysis of Spatospectral Lobes in High-Performance Aircraft Jet Noise." *AIAA J.*, Vol. 59, No. 10, 2021, pp. 4166–4178.
- [10] Oertel, H. "Measured Velocity Fluctuations Inside the Mixing Layer of a Supersonic Jet." *Recent Contributions to Fluid Mechanics*, Vol. 1, 1982, pp. 170–179.
- [11] Tam, C. K. W., and Hu, F. Q. "On the Three Families of Instability Waves of High-Speed Jets." *J. Fluid Mech.*, Vol. 201, 1989, pp. 447–483.
- [12] Seiner, J. M., Ponton, M. K., Jansen, B. J., and Lagen, N. T. "The Effects of Temperature on Supersonic Jet Noise Emission." *AIAA Paper 92-02-046*, 1992.
- [13] Greska, B. J. *Supersonic Jet Noise and Its Reduction Using Microjet Injection*. Ph.D. Dissertation. Florida State University, 2005.
- [14] James, M. M., Salton, A. R., Gee, K. L., Neilsen, T. B., McNerny, S. A., and Kenny, R. J. "Modification of Directivity Curves for a Rocket Noise Model." *Proc. Mtgs. Acoust.*, Vol. 18, 2012.
- [15] Hart, G. W., Mathews, L. T., Anderson, M. C., Durrant, T., Bassett, M. S., Olausson, S. A., Houston, G., and Gee, K. L. "Methods and Results of Acoustical Measurements Made of a Delta IV Heavy Launch." *Proc. Mtgs. Acoust.*, Vol. 45, 2021.
- [16] Bassett, M. S., Gee, K. L., Hart, G. W., Mathews, L. T., Rasband, R. D., and Novakovich, D. J. "Peak Directivity Analysis of Far-Field Acoustical Measurements during Three GEM 63 Static Firings." *Proc. Mtgs. Acoust.*, Vol. 39, 2019.
- [17] Mathews, L. T., Gee, K. L., and Hart, G. W. "Characterization of Falcon 9 Launch Vehicle Noise from Far-Field Measurements." *J. Acoust. Soc. Am.*, Vol. 150, 2021, pp. 620–633.
- [18] Murray, N. E., and Lyons, G. W. "On the Convection Velocity of Source Events Related to Supersonic Jet Crackle." *J. Fluid Mech.*, Vol. 793, 2016, pp. 477–503.
- [19] Tam, C. K. W., and Parrish, S. A. "Noise of High-Performance Aircraft at Afterburner." *Journal of Sound and Vibration*, Vol. 352, 2015, pp. 103–128.
- [20] Chen, S., Gojon, R., and Mihaescu, M. "Flow and Aeroacoustic Attributes of Highly-Heated Transitional Rectangular Supersonic Jets." *Aerospace Science and Technology*, Vol. 114, 2021, p. 106747.
- [21] Leete, K. M., Vaughn, A. B., Bassett, M. S., Rasband, R. D., Novakovich, D. J., Gee, K. L., Campbell, S. C., Mobley, F. S., and Wall, A. T. "Jet Noise Measurements of an Installed GE F404 Engine." *AIAA Paper 2021-1638*, 2021.
- [22] Gee, K. L., Neilsen, T. B., and James, M. M. "Including Source Correlation and Atmospheric Turbulence in a Ground Reflection Model for Rocket Noise." *Proc. Mtgs. Acoust.*, Vol. 22, 2014.

- [23] Christian, M. A., Gee, K. L., Streeter, J. B., Mathews, L. T., Wall, A. T., Johnson, J. P., and Campbell, S. C. “Installed F404 Noise Radiation Characteristics from Far-Field Measurements.” *AIAA Paper 2022-3027*, 2022.
- [24] Tam, C. K. W. “Mach Wave Radiation from High-Speed Jets.” *AIAA J.*, Vol. 47, No. 10, 2009, pp. 2440–2448.
- [25] Greska, B., Krothapalli, A., Horne, W. C., and Burnside, N. “A Near-Field Study of High Temperature Supersonic Jets.” *AIAA Paper 2008-3026*, 2008.
- [26] Leete, K. M., Gee, K. L., Liu, J., and Wall, A. T. “Near-Field Acoustical Holography and Acoustic Power Analysis of a Simulated, Highly Heated Supersonic Jet.” *J. Acoust. Soc. Am.*, Vol. 151, No. 3, 2022, pp. 1989–2001.
- [27] Gee, K. L., Akamine, M., Okamoto, K., Neilsen, T. B., Cook, M. R., Tsutsumi, S., Teramoto, S., and Okunuki, T. “Characterization of Supersonic Laboratory-Scale Jet Noise with Vector Acoustic Intensity.” *AIAA Paper 2017-3519*, 2017.
- [28] Mathews, L. T., Gee, K. L., Olaveson, T., and Wall, A. T. Acoustic Source Characterization and Decomposition of an Installed GE F404 Engine Using Near-Field Acoustical Holography. Presented at the 2023 AIAA Aviation and Aeronautics Forum and Exposition, 2023.